Supplementary Information

Triboelectric Charge-Enhanced Rolling-Structured Triboelectric Nanogenerator via Ternary Triboelectric Interface for Wave Energy Harvesting and Marine Sensing

Yuwei Ma[a, b], Mengfan Li[a, b], Ying Lou[a, b], Jiaxi Hu[a, c], Guangli Zhang[a, c], Yaya Xu[a, c], Aifang Yu[a, b, c, *], and Junyi Zhai[a, b, c, *]

[a]Beijing Key Laboratory of Micro-Nano Energy and Sensor, Center for High-Entropy Energy and Systems, Beijing Institute of Nanoenergy and Nanosystems, Chinese Academy of Sciences, Beijing 101400, P. R. China

[b]School of Nanoscience and Engineering, University of Chinese Academy of Sciences, Beijing 100049, China

[c]Center on Nanoenergy Research, Institute of Science and Technology for Carbon Peak & Neutrality; Key Laboratory of Blue Energy and Systems Integration (Guangxi University), Education Department of Guangxi Zhuang Autonomous Region; School of Physical Science & Technology, Guangxi University, Nanning 530004, China

*Corresponding authors at: Beijing Key Laboratory of Micro-Nano Energy and Sensor, Center for High-Entropy Energy and Systems, Beijing Institute of Nanoenergy and Nanosystems, Chinese Academy of Sciences, Beijing 10l400, P. R. China

E-mail addresses: yuaifang@binn.cas.cn (A. Yu), jyzhai@binn.cas.cn (J. Zhai).

Table S1. Comparison of the output characteristics between this work and previous devices.[1, 2]

Device	Volume	Peak Power Density	Average Power Density	Matched Impedance	Ref
RS-TENG	3.1×10^{-4} m^3	52.87 $W\cdot m^{-3}$	10.08 $W\cdot m^{-3}$	500 MΩ	[1]
Self-assembly TENG	2.68×10^{-4} m^3	32.6 $W\cdot m^{-3}$	8.69 $W\cdot m^{-3}$	1 GΩ	[2]
TCE-TENG	3.2×10^{-3} m^3	67.2 $W\cdot m^{-3}$	21 $W\cdot m^{-3}$	100 MΩ	**This Work**

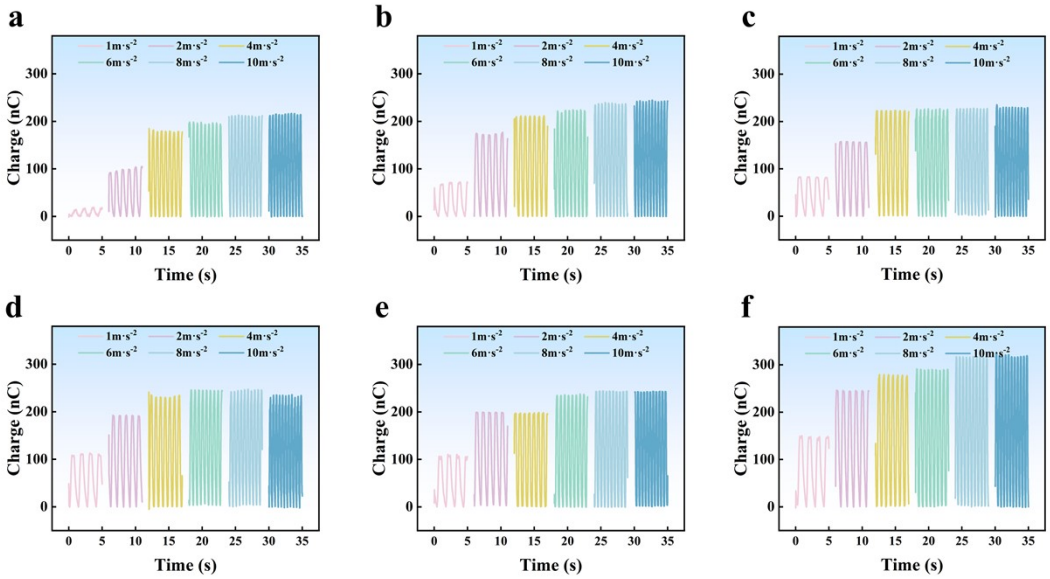

Fig. S1 The transferred charge of the single-layer TENGs. (a) PVC/Cu. (b) PVC/Cu/POM. (c) PA/Cu. (d) PA/Cu/PTFE. (e) PTFE/Cu. (f) PTFE/Cu/POM.

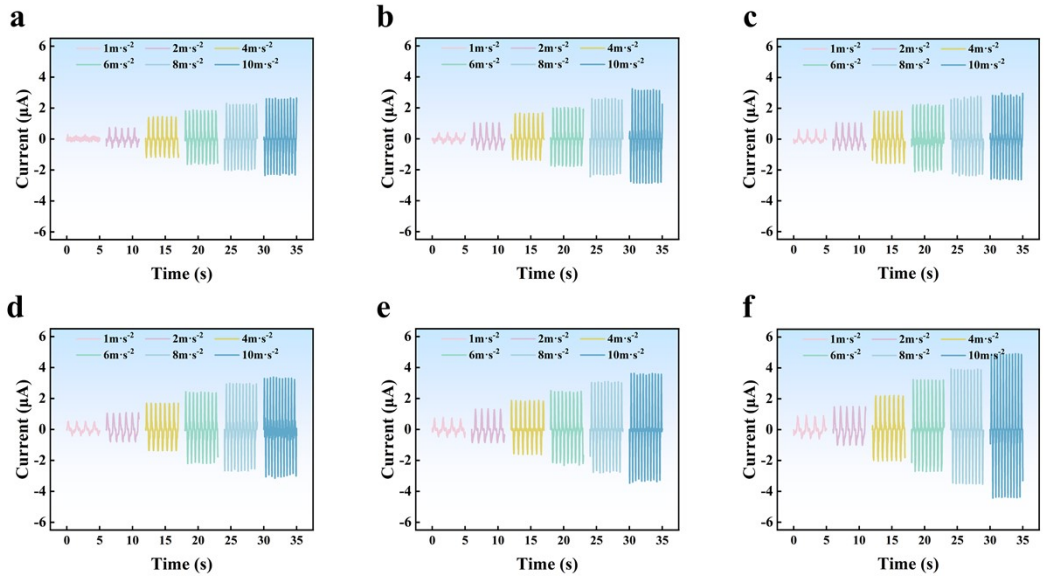

Fig. S2 The short-circuit current of the single-layer TENGs. (a) PVC/Cu. (b) PVC/Cu/POM. (c) PA/Cu. (d) PA/Cu/PTFE. (e) PTFE/Cu. (f) PTFE/Cu/POM.

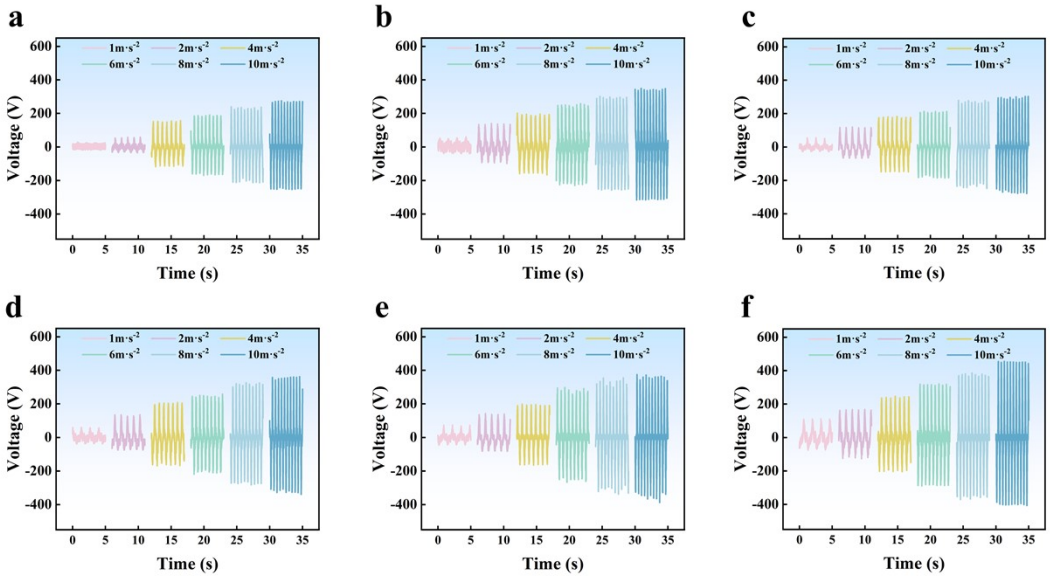

Fig. S3 The open-circuit voltage of the single-layer TENGs. (a) PVC/Cu. (b) PVC/Cu/POM. (c) PA/Cu. (d) PA/Cu/PTFE. (e) PTFE/Cu. (f) PTFE/Cu/POM.

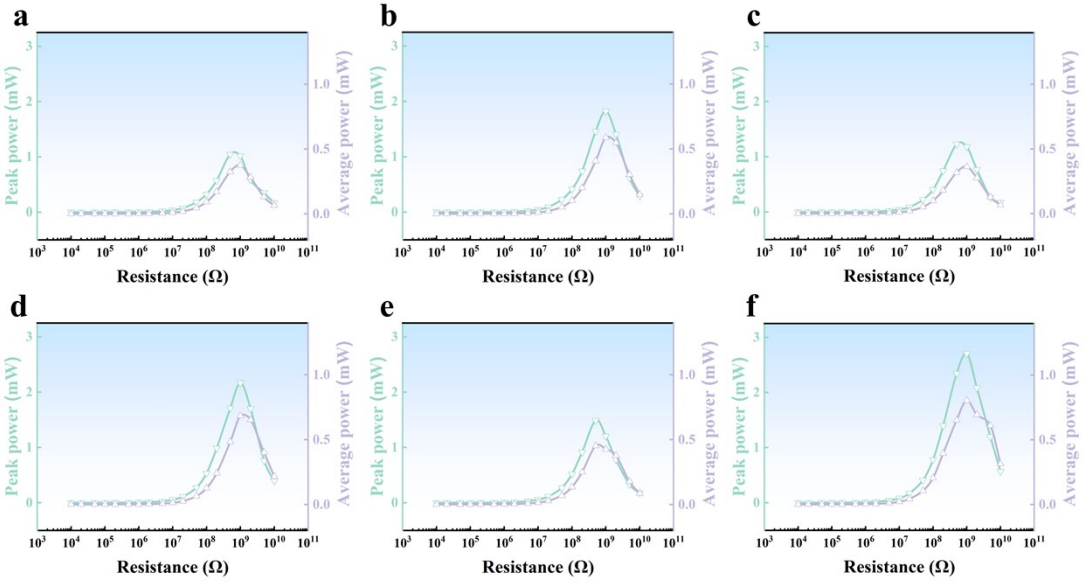

Fig. S4 The peak and average power of the single-layer TENGs. (a) PVC/Cu. (b) PVC/Cu/POM. (c) PA/Cu. (d) PA/Cu/PTFE. (e) PTFE/Cu. (f) PTFE/Cu/POM.

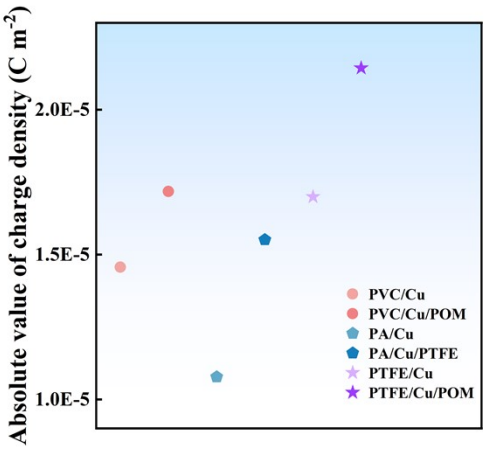

Fig. S5 Faraday cup–derived surface charge density of dielectric spheres from six TENG devices after sufficient operation cycles.

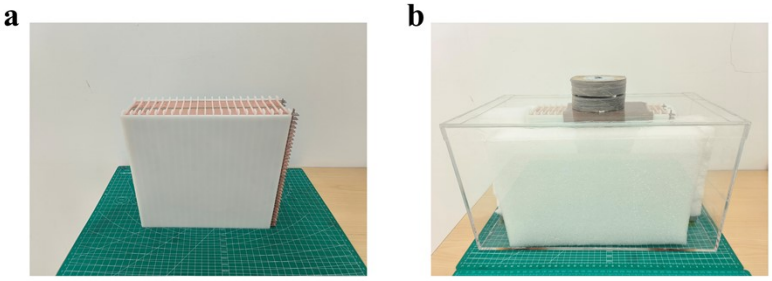

Fig. S6 (a) Photograph of the TCE-TENG. (b) Photograph of the TCE-TENG encapsulated within an acrylic box.

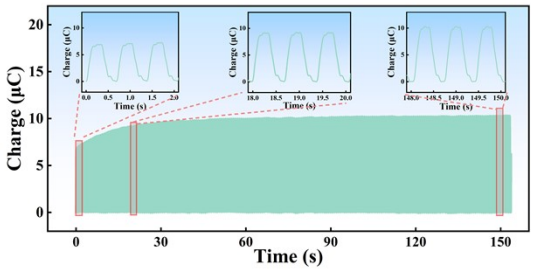

Fig. S7 The transferred charge accumulation process upon initial mechanical excitation.

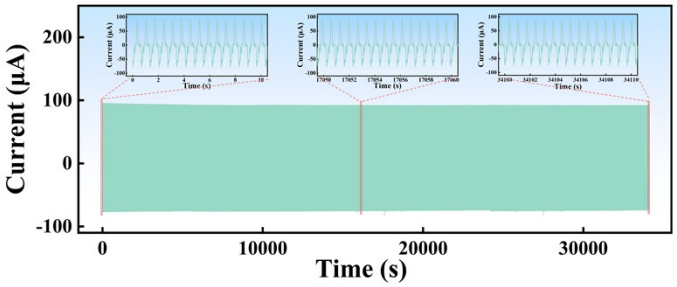

Fig. S8 The long-term stability test of the TCE-TENG.

Fig. S9 Photograph of the laboratory wave generator.

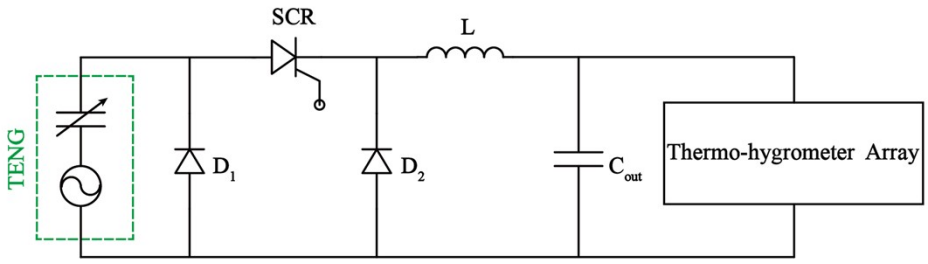

Fig. S10 Circuit Diagram of the TCE-TENG Powering a Temperature and Humidity Sensor Array through the PMC.

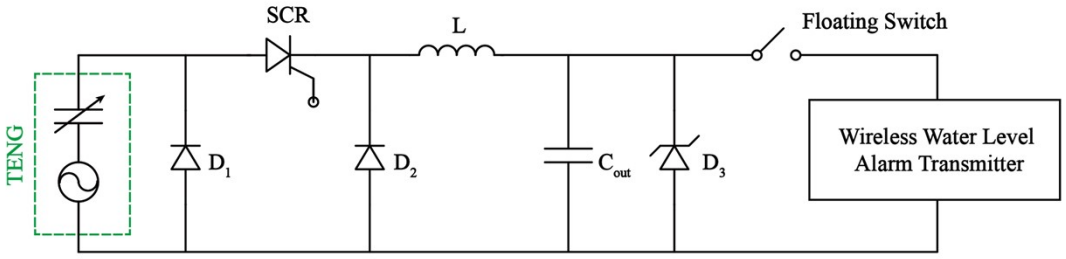

Fig. S11 Circuit Diagram of the TCE-TENG Powering a water level alarm system through the PMC.

References

1. Y. X. Duan, H. X. Xu, S. J. Liu, P. F. Chen, X. Y. Wang, L. Xu, T. Jiang and Z. L. Wang, Nano Res., 2023, 16, 11646-11652.

2. X. D. Yang, L. Xu, P. Lin, W. Zhong, Y. Bai, J. J. Luo, J. Chen and Z. L. Wang, Nano Energy, 2019, 60, 404-412.